PRODUCTION AND ANALYSIS OF POLYGON PROFILES

By

E. FILEMON

DEPARTMENT II FOR TECHNICAL MECHANICS, POLYTECHNIC UNIVERSITY, BUDAPEST

(Received September 18 1958)

Introduction

Connection between shaft and hub is generally secured through keying, the shaft end being splined or shaped to some other profile and fitted in a hole. Modern machine construction endeavours to solve the problem of con-

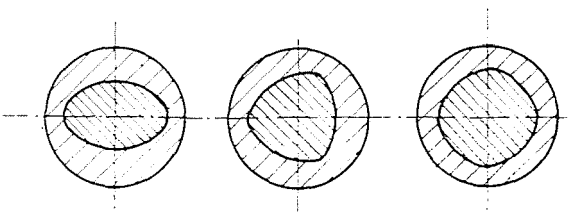

Fig. 1

nection between shaft and hub by fitting profiled pins and holes. In 1939, the firm E. Krause and Co. developed a machine for the production of triangular profiles with filleted corners, the so-called K profiles. This machine serves for processing, both external and internal surfaces of K profiles. In our days such machine tools have been developed on which profiles flanked by arcs with any desired number of angles, and filleted corners, the so-called polygon profiles can be produced (Fig. 1).

The present paper offers a comprehensive analysis of various polygon profiles starting from the kinematic sketch of the above-mentioned machine, describing techniques for generating polygon profiles, and in conclusion points out. how polygon profiles can be produced by means of an equipment which can be mounted upon a common grinding machine in hand.

Analysis of polygon profiles

The analysis of polygon profiles can be approached by examining the operation of the machine. The kinematic sketch of the machine is given in

Fig. 2. Grinding of the workpiece (8) is done by the grinding disc (1), the axis of which executes simultaneous horizontal and vertical motions during operation. The motions in both directions of the grinding disc are commanded by an eccentric disc (4), the eccentricity e of which is adjustable according to the profile wanted. The eccentric controls the horizontal motion of the grinding disc shaft through the slide (3) directly, and the vertical motion of the same indirectly, through the two-arm lever (7) with a regulable

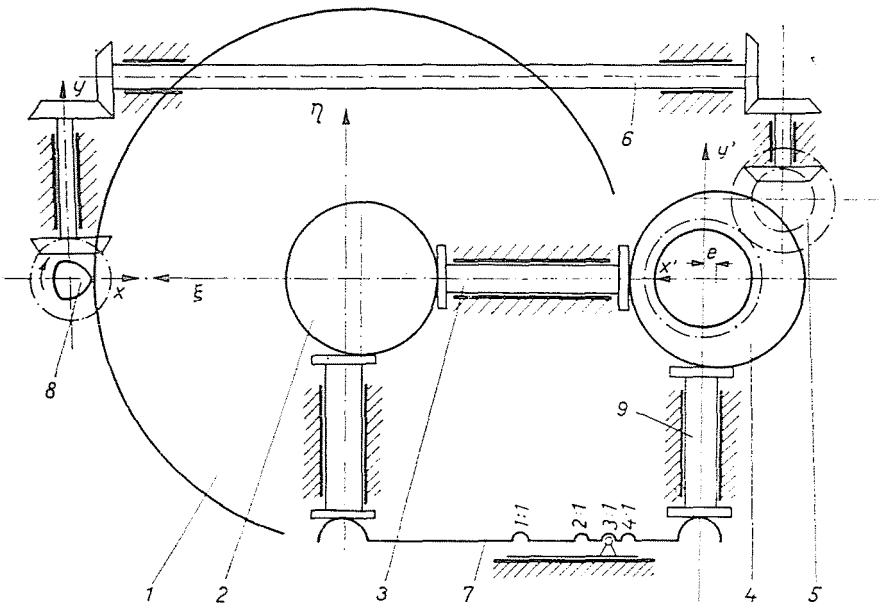

Fig. 2

fulcrum. As a result of the simultaneous horizontal and vertical motions of the center of the disc, this center moves along a specified curved path.

In the following the equation of the path of the disc center will be developed, from which the equation of the profile to be generated on the workpiece can be derived.

Curved path of disc center

Fig. 3 shows the eccentric (4). The center of rotation of the eccentric is O', its geometrical center moving along a circle of the radius e is C. Turn the eccentric from the position shown in the figure by an angle β, then the center C comes to position C'. Co-ordinates of the point C' are :

$$x' = e \cos \beta$$

$$y' = e \sin \beta$$

Members (3) and (9) terminate in flat sides perpendicular to their directions of motion, therefore, their displacements correspond to the co-ordinates of the point C', respectively.

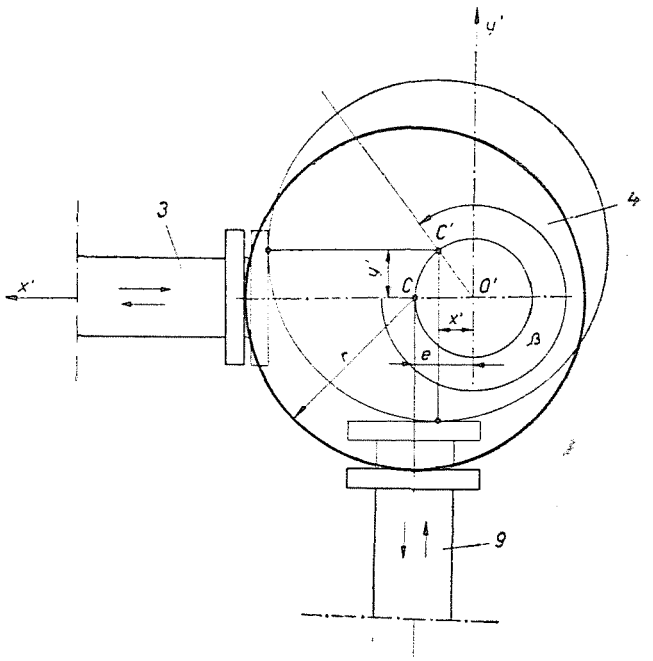

Fig. 3

Denoting the transmission ratio of the member (7) by k, in a new co-ordinate system ξ, η, shifted in respect to the first one to a constant distance, the co-ordinates of the grinding disc center will be (Fig. 2):

$$\xi = x' \tag{1}$$

$$\eta = k\ y' \tag{2}$$

or, after reduction

$$\frac{\xi^2}{e^2} + \frac{\eta^2}{k^2 e^2} = 1 \tag{3}$$

As can be seen, the resultant of the two harmonic motions along two axes perpendicular to each other causes the center of the disc to move along an ellipse, the minor axis of which is *2e*, and major axis *2ke*.

The insertion of the gear (5) between workpiece and driving eccentric causes the center of the disc to make the swinging motion examined above,

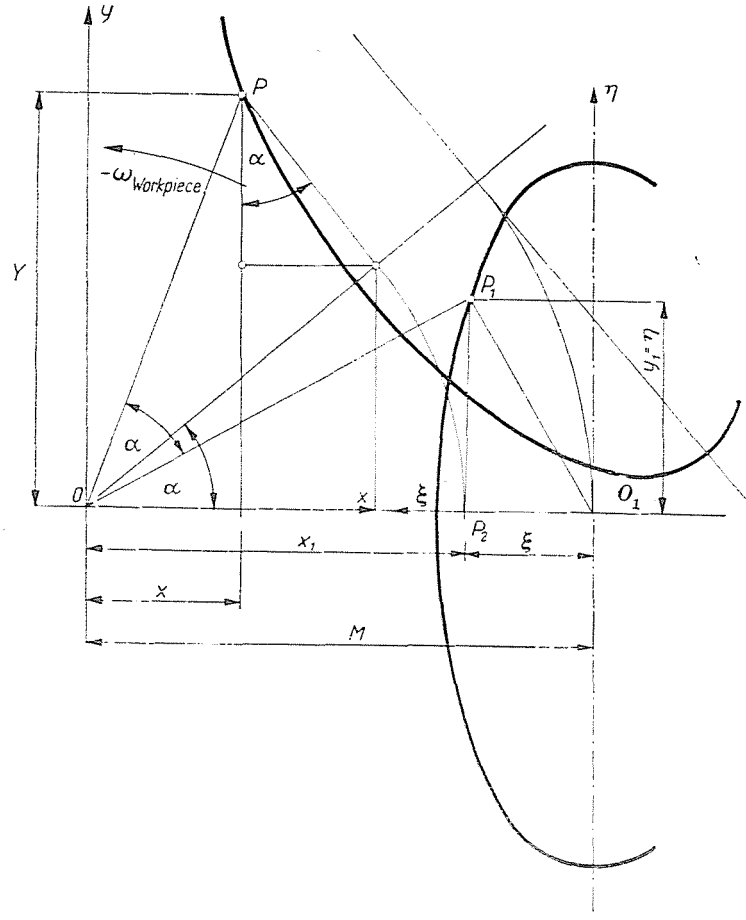

Fig. 4

n times by each revolution of the workpiece — where *n* is the ratio of the numbers of revolutions of the workpiece and the eccentric, *i. e.* the transmission ratio. Polygon profiles fit for use in practice will be obtained, of course, only if *n* is a positive integer number, also denoting the number of angles of the polygon.

Fig. 4 shows the curved path of the grinding disc center in case of the proportionality factor of the lever arms is *k*.

Supposing the whole system is rotating at an angular velocity equal to that of the workpiece but of opposed sign. As a consequence, the workpiece comes to a still-stand, while point O_1, Fig. 4 rotates about the axis of the workpiece. Now the equation for the path of the grinding disccenter may be written. For this purpose the co-ordinates according to Eqs. (1) and (2) can be used. Denoting the distance $\overline{OO_1}$, Fig. 4 by M, we can write the equation of the ellipse corresponding to Eq. (3) in a system of co-ordinates x, y attached to the center of the workpiece (Fig. 4), as

$$x_1 = M - e \cos \beta$$

$$y_1 = k\ e \sin \beta$$

Let the transmission ratio between the numbers of revolution of the workpiece and driving eccentric, respectively, be n, the angular displacement of the eccentric β, and the angular displacement of the workpiece α: then the following relationship between β and α holds true:

$$\beta = n\alpha \tag{4}$$

Taking this into consideration

$$x_1 = M - e \cos n\alpha \tag{5}$$

$$y_1 = k\ e \sin n\alpha \tag{6}$$

While the eccentric turns away with an angle β, the center of the grinding disc arrives at point P_1 (Fig. 4). The workpiece at the same time turns through an angle α; from this follows that by the application of the principle of reciprocity of motions, the center of the grinding disc comes to point P. This point can be determined by turning off the triangle OP_1P_2 by an angle α.

The co-ordinates of point P in the system of co-ordinates x, y are:

$$X = x_1 \cos \alpha - y_1 \sin \alpha$$

$$Y = x_1 \sin \alpha + y_1 \cos \alpha$$

Substitution of x_1 and y_1 from Eqs. (5) and (6) gives the parametric equation of the path of the grinding disc center as a function of the angular displacement of the workpiece:

$$X = M \cos \alpha - e \cos \alpha \cos n\alpha - k\ e \sin n\alpha \sin \alpha \tag{7}$$

$$Y = M \sin \alpha - e \sin \alpha \cos n\alpha + k\ e \sin n\alpha \cos \alpha \tag{8}$$

The curve determined by Eqs. (7) and (8) is the path of the grinding disc center. Reverting to the derivation of this curve, out of all the curves of the set obtained by varying the proportionality factor of the lever arms, we can select the one which is the most advantageous from the point of view of production, as well as of the connection of the members.

Let the center of the grinding disc lie at point A, Fig. 5, when the driving eccentric turns in an angle $n\alpha$. The workpiece in the meanwhile turns in an angle α, thus, relatively to the workpiece at stillstand, point A gets into position A'.

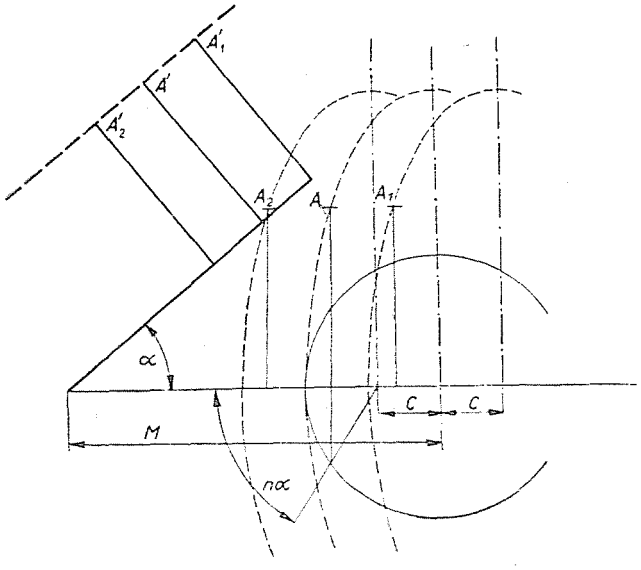

Fig. 5

Imagine the workpiece and the axis of the grinding disc moving away from each other, *i.e.* the constant M which occurs in the equation increasing ($M_1 = M + c$). Then point A comes to A_1, and point A'_1 will be obtained by drawing a perpendicular at a distance $M + c$ to the straight line inclined at an angle α, mentioned above and measuring the distance $k\,e \sin n\alpha$ upon it.

Similarly, in the case $M_2 = M - c$ the center of the disc comes to the point A'_2. Fig. 5 demonstrating that if the straight line drawn through points A'_2 A' A'_1 is perpendicular to the profile at the points A'_2, A' and A'_1, the three curves containing the points under consideration are equidistant. These curves may be treated in such a way, that the center of the grinding disc lies at point A and the radius of the disc is c : thus, the grinding disc comes into contact with the workpiece at point A'_2 in the case of processing a shaft,

and at point A_1' in the case of grinding a hole (Fig. 6). If the straight line of A_2', A', A_1' is normal to the profile, the tangent to the profile will be perpendicular to this straight line, and as a consequence, the common tangent of the profile and disc is parallel to the major axis of the elliptical path of the disc center. Thus final processing is done through the point of the disc which is cut away from its mantle by a straight line parallel to the minor axis, passing through the center of the disc.

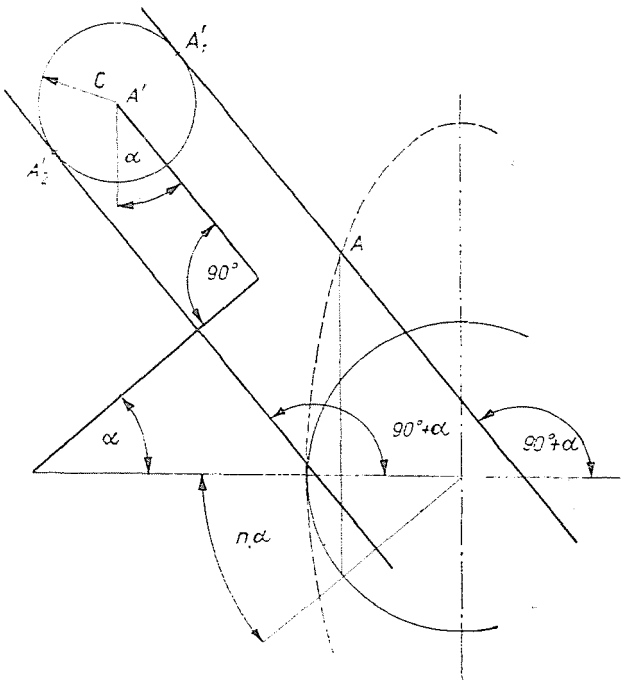

Fig. 6

All this holds true in case the tangent to the profile includes an angle $(90° + \alpha) = \varphi$ with the positive axis x.

The direction of the tangent to the profile is given by

$$\operatorname{tg}\varphi = \frac{dY}{dX} = Y'$$

since

$$Y' = \frac{\dot{Y}}{\dot{X}},$$

and

$$\dot{Y} = \frac{dY}{d\alpha} = M\cos\alpha - e\cos\alpha\cos n\alpha(1-kn) + e\sin\alpha\sin n\alpha(n-k) \quad (9)$$

$$\dot{X} = \frac{dX}{d\alpha} = -M\sin\alpha + e\sin\alpha\cos n\alpha(1-kn) + e\cos\alpha\sin n\alpha(n-k) \quad (10)$$

Substituting

$$\operatorname{tg}\varphi = \frac{M\cos\alpha - e\cos\alpha\cos n\alpha(1-kn) + e\sin\alpha\sin n\alpha(n-k)}{-M\sin\alpha + e\sin\alpha\cos n\alpha(1-kn) + e\cos\alpha\sin n\alpha(n-k)}$$

it can be seen that the relationship $\varphi = 90^\circ + \alpha$ holds true when $n = k$, namely, in this case

$$\operatorname{tg}\varphi = -\operatorname{cotg}\alpha \quad (11)$$

since

$$-\operatorname{cotg}\alpha = \operatorname{cotg}(-\alpha) = \operatorname{tg}(90^\circ + \alpha)$$

thus

$$\operatorname{tg}\varphi = \operatorname{tg}(90^\circ + \alpha)$$

i.e.

$$\varphi = 90^\circ + \alpha$$

It has been proved by this, that the profile is always determined by the point which is cut away from the mantle of the grinding disc by the straight line passing through the center of the disc parallelly to the minor axis of the elliptical path of the disc center. It is easy to see that the contact is brought about along a curve identical with the path of the center, yet shifted to the distance c (Fig. 7).

When writing the equation of the profile generated on the workpiece, Eqs. (7) and (8) are modified only in so far as the place of the constant M is taken by $M - c$.

As the minimum dimension of the workpiece (diameter of the inner tangent circle to the profile) is determined by point a, and the maximum dimension (diameter of the outer tangent circle) by point b (Fig. 7), the constant $M - c$ occurring in the equation is identical to the half of the mean diameter R of the profile,

$$R = \frac{r_{\max} + r_{\min}}{2} \quad (12)$$

At the same time $2R$ is the nominal diameter of the profile.

When $k \neq n$ then $\varphi \neq 90° + \alpha$, as a consequence the curves are not equidistant, and the diameter of the disc influences both the configuration and the size of the profile. The equation of the profile does not coincide with that of the path of the grinding disc center.

According to the above, in case $k = n$ the equation of the profile becomes

$$x = R \cos \alpha - e \cos \alpha \cos n\alpha - n\, e \sin n\alpha \sin \alpha \tag{13}$$

$$y = R \sin \alpha - e \sin \alpha \cos n\alpha + n\, e \sin n\alpha \cos \alpha \tag{14}$$

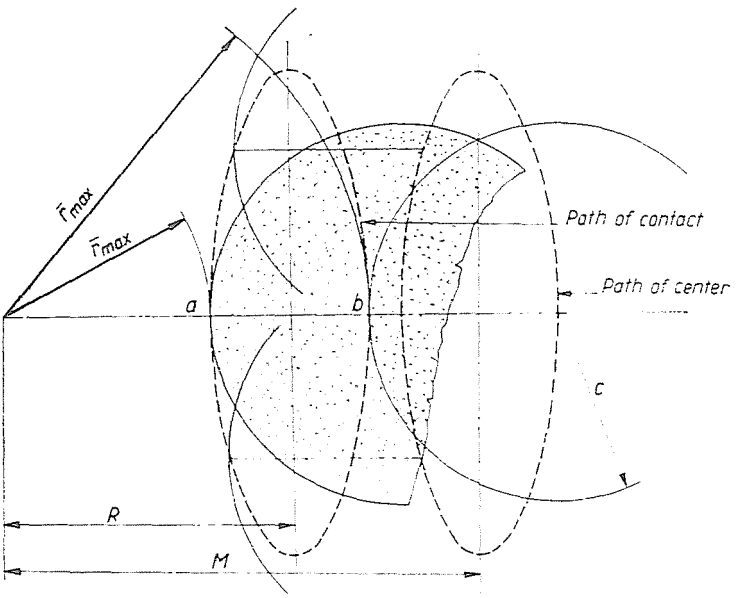

Fig. 7

An analysis of the path of the grinding disc center advocates similarly for the condition $k = n$.

A preliminary construction also shows that the curve corresponding to the condition $k = n$ goes the innermost path and thus has the shortest arc. The correctness of this statement can be checked mathematically.

The equation determining the length of the arc of the curve is

$$\varrho\, d\alpha = di = \sqrt{dX^2 + dY^2}$$

where ϱ denotes the radius of curvature connected to the respective points on the curve,

di is the elementary arc length belonging to the angular displacement $d\alpha$. Since

$$\dot{X} = \frac{dX}{d\alpha} \text{ and } \dot{Y} = \frac{dY}{d\alpha}$$

hence, substituting $\dot{X}$ and $\dot{Y}$ from Eqs. (9) and (10)

$$dX = [-M \sin \alpha + e \sin \alpha \cos n\alpha \ (1-kn) + e \sin n\alpha \cos \alpha (n-k)] \, d\alpha$$

$$dY = [\ M \cos \alpha - e \cos \alpha \cos n\alpha \, (1-kn) + e \sin n\alpha \sin \alpha \ (n-k)] \, d\alpha$$

and performing the operations indicated

$$di = \sqrt{[M - e \cos n\alpha \, (1 - kn)]^2 + e^2 \sin^2 n\alpha \, (n - k)^2} \, d\alpha$$

thus the circumference

$$i = \int_0^{2\pi} \sqrt{[M - e \cos n\alpha \, (1 - kn)]^2 + e^2 \sin^2 n\alpha \, (n - k)^2} \, d\alpha \qquad (15)$$

The computation proves the correctness of the construction, since the second term of the radical is positive in any case, consequently the smallest circumference will be obtained when the factor of proportionality of the lever is equal to the gear ratio between workpiece and driving eccentric. Then $n = k$, hence

$$e^2 \sin^2 n\alpha \ (n-k)^2 = 0$$

and according to the above, if $k = n$ the constant M occurring in the equation is equal to the mean radius of the profile ($M = R$), thus the circumference becomes

$$i = \int_0^{2\pi} [R - e \cos n\alpha \, (1 - n^2)] \, d\alpha \qquad (16)$$

integrating

$$i = \left[R\alpha - \frac{e \, (1 - n^2)}{n} \sin n\alpha \right]_0^{2\pi}$$

and taking the limits into consideration

$$i = 2R\pi \qquad (17)$$

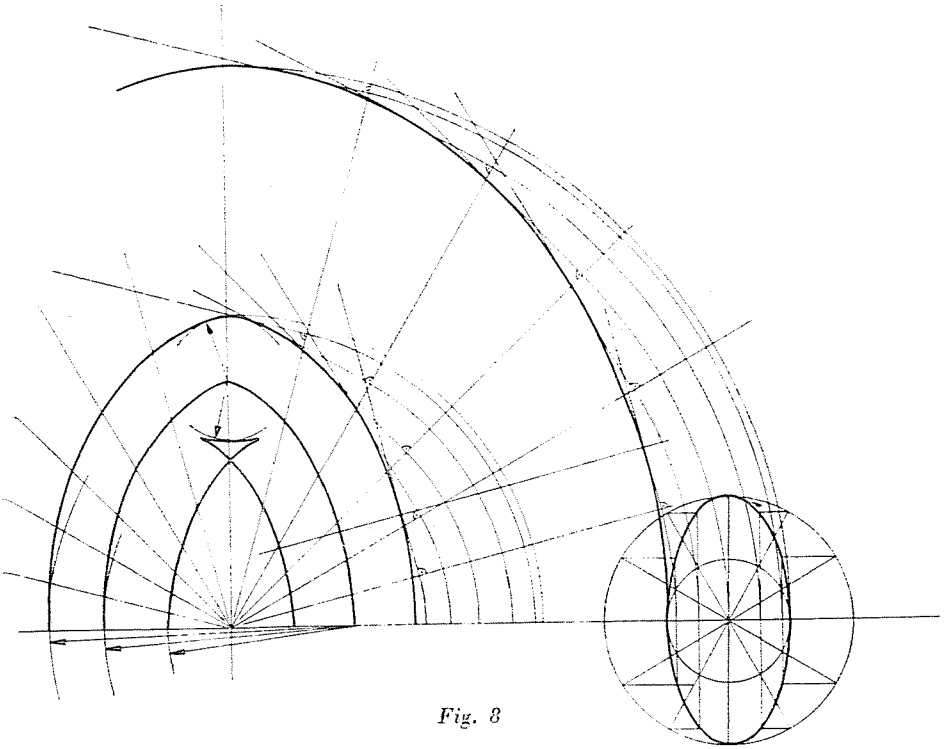

Fig. 8

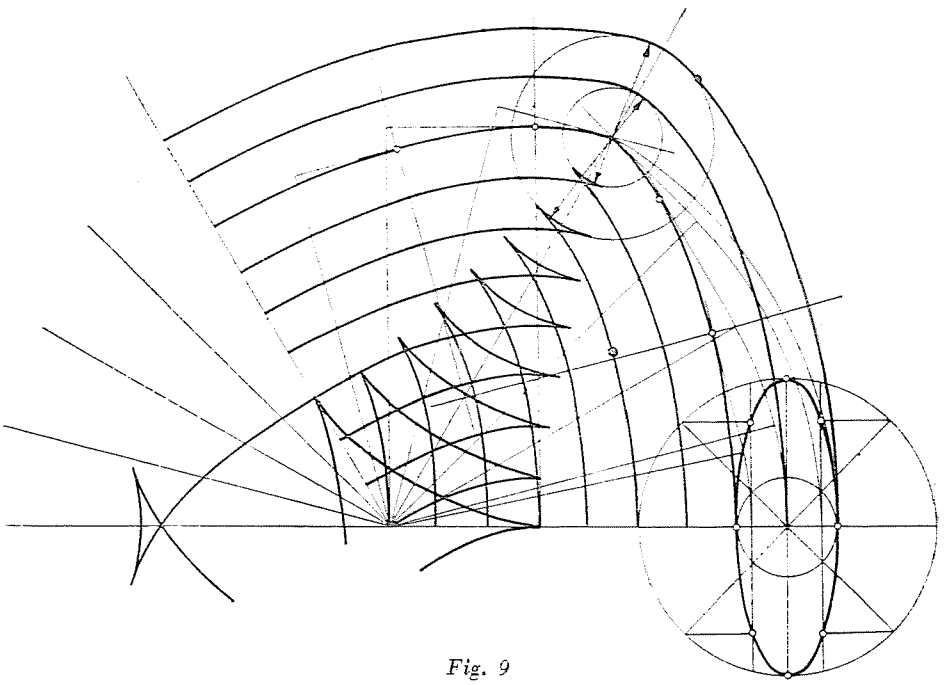

Fig. 9

The result is worthy of attention: in case $k = n$ the circumference is independent both of the number of angles and the eccentricity, being equal to the circumference of the circle of nominal diameter. The case $k = n$ is the most favourable also, according to this consideration, since, other things being equal, the shortest curve also implies the shortest time for processing.

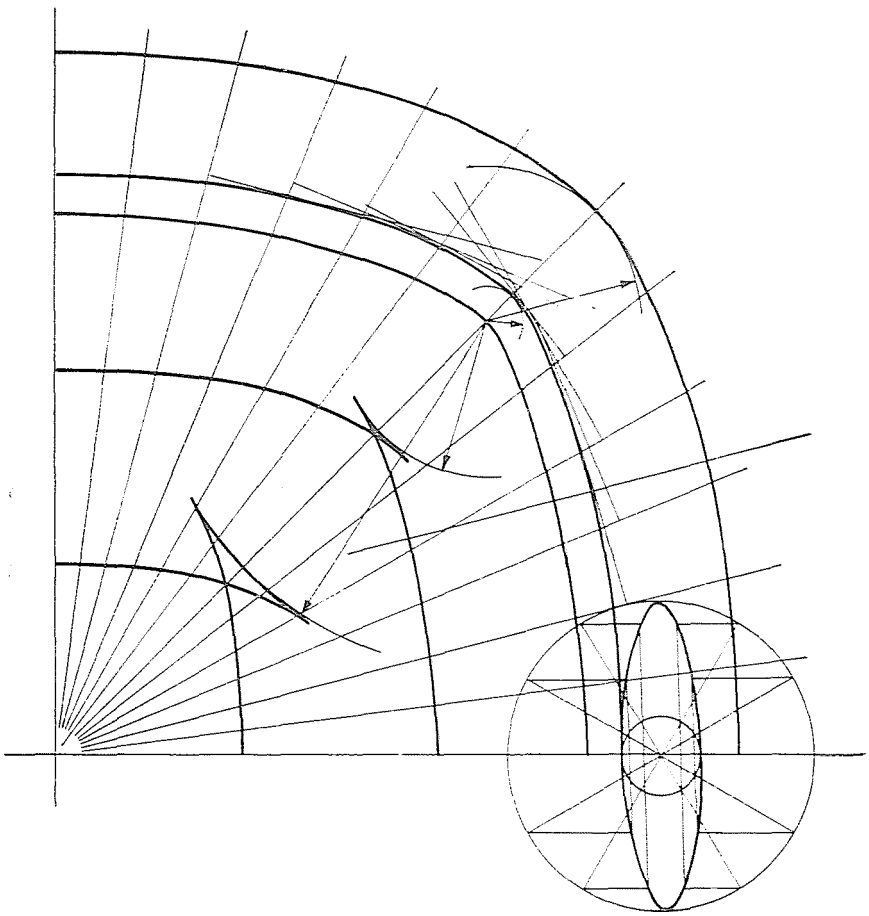

Fig. 10

As can be seen the selection of a value $k = n$ is justified. In the following this particular case will be analysed. Since it is known that contact is brought about along an elliptical curve, it can be stated that the radius of the profile will be minimum at the instant when the angular displacement of the eccentric is $\beta = 0° + 2a\pi$ (where a is an integer number, $0 < a \leq n$), and maximum, when $\beta = 180° + 2a\pi$. From the relationship between the angular displacement α of the workpiece and angular displacement of the

eccentric follows that $\alpha = \frac{0° + 2a\pi}{n}$ at r_{min} and $\alpha = \frac{180° + 2a\pi}{n}$ at r_{max}. It can be laid down as a fact, furthermore, that for a profile of n angles, suitable for the connection of machine parts the number of the limit values is $2n$.

Polygon profiles constructed according to the method outlined above, with constant eccentricity e and number of angles n. but with varying mean diameter are shown: in Fig. 8 for $n = 2$, Fig. 9 for $n = 3$ and Fig. 10 for $n = 4$.

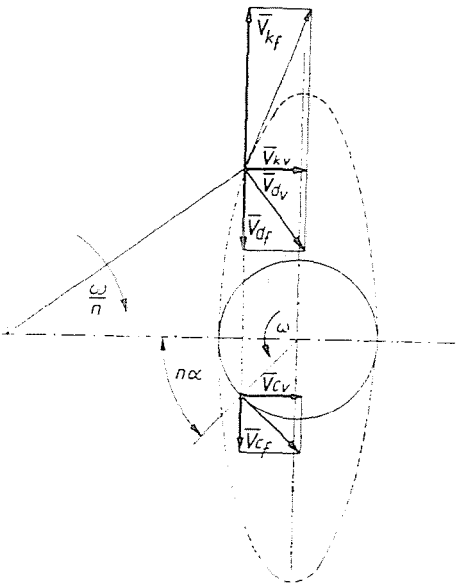

Fig. 11

Examination of these figures shows that in case of reducing the diameter (or, which comes to the same thing, of increasing the eccentricity) a cusp is formed on the profile, then the profile branches intersect each other, as a consequence, a profile of a smaller diameter than wanted will be produced, since the disc cuts into the part processed during the first half swing. This fact motivates the kinematic analysis of profile generation.

Kinematic analysis of profile generation

Let the eccentric (4) rotate counterclockwise with a constant angular velocity ω. The velocity of its geometrical center is then $\bar{v}_c = e\bar{\omega}$ (Fig. 11). The center of the disc moves in a horizontal direction, with a velocity $\bar{v}_{kv}$ which is equal to the horizontal component of $\bar{v}_c$. $\bar{v}_{kv} = e\bar{\omega} \sin n\alpha$. In a vertical direction the velocity is multiplied by the gear ratio of the lever,

$\bar{v}_{kf} = -n\bar{v}_{cf}$. In case we consider the vector $\bar{v}_{cf}$ pointing downward as negative, then $\bar{v}_{kf} = \text{ne } \bar{\omega} \cos n\alpha$.

The workpiece rotates clockwise with an angular velocity $\frac{\omega}{n}$. The velocity components of the point which is in contact with the grinding disc are: horizontal $\bar{v}_{dv} = ne \sin n\alpha \frac{\omega}{n} = e\,\bar{\omega} \sin n\alpha$, vertical $\bar{v}_{df} = \frac{\omega}{n}(R + e \cos n\alpha)$.

It can be seen that in case of any chosen angle n the horizontal velocity component of the points in contact on disc and workpiece are identical: $\bar{v}_{kv} = \bar{v}_{dv}$. A relative motion between disc and workpiece is possible in a

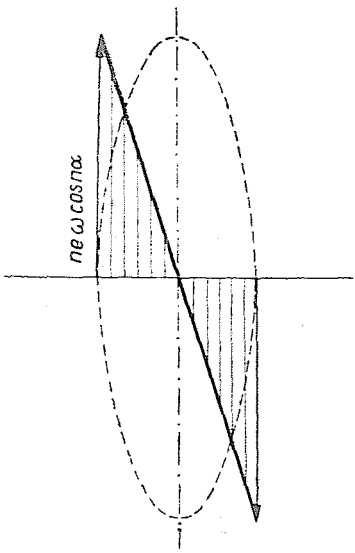

Fig. 12

vertical direction only. Therefore we can confine our investigation to the analysis of the variation of vertical components of velocity.

$\bar{v}_{kf} = n\, e\, \bar{\omega} \cos n\alpha$ as a function of the horizontal stroke of magnitude $2e$ displays a linear distribution (Fig. 12). $\bar{v}_{df} = (R + e \cos n\alpha) \frac{\bar{\omega}}{n}$ as a function of the radius also varies linearly.

Fig. 13 shows both velocity distributions. It can be seen that processing throughout the part of the stroke extending from O to e is continuous, since the disc and workpiece move convergently. Through the part from e to $2e$ the two velocities are of identical direction, thus processing is subjected to the condition that the velocity of the point on the workpiece is the higher one, failing which the disc slips forward, loses contact with the workpiece and processing comes to an end. In the second half of the stroke, begin-

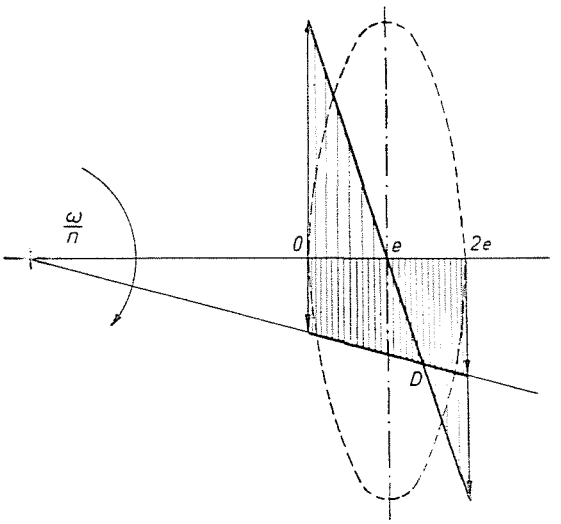

Fig. 13

ning from the point of intersection of the velocity distribution curve (point *D*) the disc has a no-load run.

As is seen, a condition of continuous processing is that velocity distribution curves resulting from the rotation of the workpiece and swinging motion of the disc should not intersect each other on the section of mag-

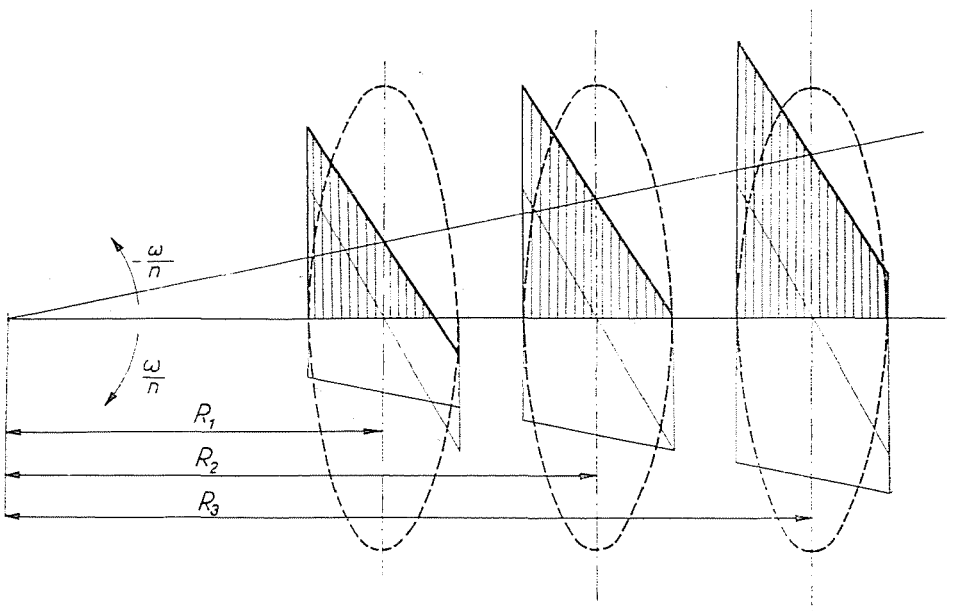

Fig. 14

nitude $2e$ of the stroke. In a limitation case maximum velocity of the workpiece is equal to the velocity resulting from the swinging motion of the disc.

$$(R + e)\frac{\omega}{n} = n\, e\, \omega \tag{18}$$

Fig. 14 shows three variants of velocity distribution curves with eccentricity e a constant and radii R varying. Rotate the whole system with an

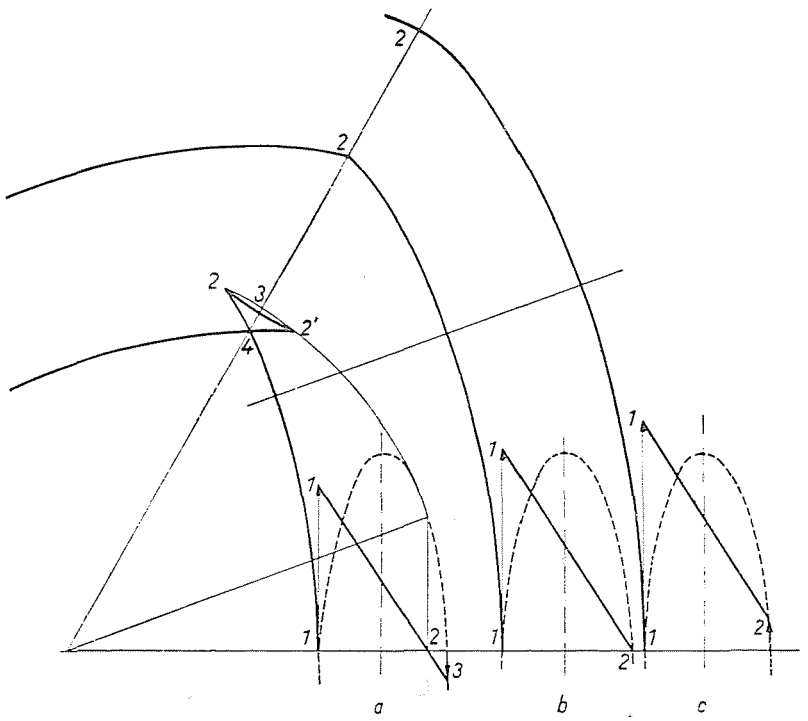

Fig. 15

angular velocity $-\frac{\omega}{n}$. The workpiece comes to a stillstand, while the disc continues performing its swinging motion as described above, in a system rotating with an angular velocity $\frac{\omega}{n}$. Consequently, its velocity will be the resultant of the two motions. In Fig. 15 the variation of relative velocities are shown, also apart, for each of the three cases.

Let us by turn examine the three cases.

a) Here $(R + e)\frac{\omega}{n} < n\,e\,\omega$, thus

$$R < e\,(n^2 - 1) \tag{19}$$

relative velocity at point 2 is zero (Fig. 15a). Processing is so far undisturbed. At this point the relative velocity reverses the signs, the disc has a dead center position in respect to the workpiece and starts moving in the opposite direction, receding from the piece. Its velocity increases as far as point 3. In the meanwhile the disc performs a half swing. Throughout the rest of the motion, the absolute value of the relative velocity decreases up to point 2′ where it reverses the signs again, the stone has a second dead center position and processing begins anew. The disc cuts into the profile processed through section 1—2, as a result of which the maximum radius specified cannot possibly be executed. The maximum radius of the truncated profile is delimited by point 4.

It can be seen that in case $R < e\,(n^2-1)$ the disc has an idle stroke, the profile becomes truncated, and as a consequence of the incision, the arcs of the curve meet in an edge. The profile has a cusp and therefore is unsuitable to connection parts of machines.

b) Here $(R + e)\frac{\omega}{n} = n\,e\,\omega$, thus

$$R = e\,(n^2 - 1) \tag{20}$$

Fig. 15b shows that here the relative velocity does not reverse the signs. At point 2 the disc generates the specified maximum diameter. Relative velocity at this point is zero, *i.e.* the disc comes to a stillstand for an instant, then processing goes on without incision in the profile.

Therefore, in case $R = e\,(n^2 - 1)$ the specified maximum radius can be obtained, the disc has no idle run, but still the condition of formation of cusps on the maximum radius has to be examined.

c) Here $(R + e)\frac{\omega}{n} > n\,e\,\omega$, thus

$$R > e\,(n^2 - 1) \tag{21}$$

The relative velocity neither reverses signs, nor drops to zero, therefore neither an incision, nor an idle run or formation of cusp can occur (Fig. 15c). According to the above, on profiles suitable for connecting parts of machines, the relationship

$$R > e\,(n^2 - 1)$$

holds true.

The conclusions developed from construction can also be checked mathematically. Let us examine the extreme points of the curve.

The vector equation of the profile is

$$\bar{r} = x\,\bar{i} + y\,\bar{j} \tag{22}$$

where x and y can be substituted from Eqs. (13) and (14). For determining the extreme values the vector

$$\bar{v} = \dot{x}\,\bar{i} + \dot{y}\,\bar{j}$$

is needed. At points where the scalar product $\bar{r}\,\bar{v}$ equals zero, either $\bar{r} \perp \bar{v}$, or $\bar{v} = 0$, *i.e.* there is either an extreme value, or a dead center.

$$\bar{r}\,\bar{v} = x\dot{x} + y\dot{y}$$

Substituting $\dot{x}$ and $\dot{y}$ from Eqs. (9) and (10) and performing the operations set out, considering that $k = n$, we can write :

$$\bar{r}\,\bar{v} = \sin\ n\alpha\,[R - e\,(1 - n^2)\cos\ n\alpha]\,n\,e = 0 \tag{23}$$

The product is zero if one of the factors is zero, $ne \neq 0$. $\sin\ n\alpha = 0$ in case $\alpha = 0° + a\pi$, where a may be any chosen integer number. Thus

$$\alpha = \frac{0° + a\pi}{n}$$

which gives $2n$ extreme values. *E. g.* in case $n = 3$

$$\alpha = 0°,\ 60°,\ 120°,\ 180°,\ 240°,\ 300°.$$

Further extreme values result from the condition

$$R - e\,(1 - n^2)\cos\ n\alpha = 0$$

After transposition

$$\cos n\alpha = \frac{R}{e\,(1 - n^2)} \tag{24}$$

Let us examine three cases again.

a) when $R/e < (1 - n^2)$ [case of Eq. 19] $\cos\ n\alpha < 1$, and for each ratio of R/e there are in addition $2n$ extreme values.

b) when $R/e = (1 - n^2)$ [case of Eq. 20] $\cos n\alpha = 1$. When $\cos n\alpha = 1$, then $\sin n\alpha = 0$, thus there is no further extreme value besides those mentioned above.

c) when $R/e > (1 - n^2)$ [case of Eq. 21], $\cos n\alpha > 1$, this cannot be, consequently, no further extreme value results under this condition either.

As is seen, there are generally $4n$ extreme values, yet for $R/e = 1 - n^2$ a number of $2n$ of them will disappear. The difference in the signs between the results of the conclusions drawn from Fig. 15 and of the present discussion ($n^2 - 1$ there and $1 - n^2$ here) follows from the fact that the senses of rotation of the workpiece and eccentric are opposite.

A detailed mathematical analysis of the behaviour of the profile at extreme values is unnecessary, as the construction answers this question. Possibility of inflexion does not even occur. Minimum and maximum spots are unequivocal. *E.g.* in case of $n = 3$, the radius has minimum values at $\alpha = 0°$, $120°$, $240°$, and maximums at $\alpha = 60°$, $180°$, $300°$. Only the condition of formation of cusp needs an examination apart.

The profile has a cusp where the radius of curvature is zero. The radius of curvature can be determined from the following relationship :

$$\varrho = \frac{(1 + y'^2)^{\frac{3}{2}}}{y''}$$

since

$$y' = \frac{\dot{y}}{\dot{x}} = -\operatorname{cotg}\alpha$$

and

$$y'' = \frac{dy'}{dx} = \frac{\frac{dy'}{d\alpha}}{\frac{dx}{d\alpha}} = \frac{\dot{y}'}{\dot{x}} = \frac{-1}{R\sin^3\alpha\left[1 - \frac{e}{R}\cos n\alpha\,(1 - n^2)\right]}$$

the radius of curvature is

$$\varrho = -\left[1 - \frac{e}{R}\cos n\alpha(1 - n^2)\right]R \tag{25}$$

$\varrho = 0$ when

$$1 - \frac{e}{R}\cos n\alpha\,(1 - n^2) = 0$$

$$\cos n\alpha = \frac{R}{e\,(1 - n^2)}$$

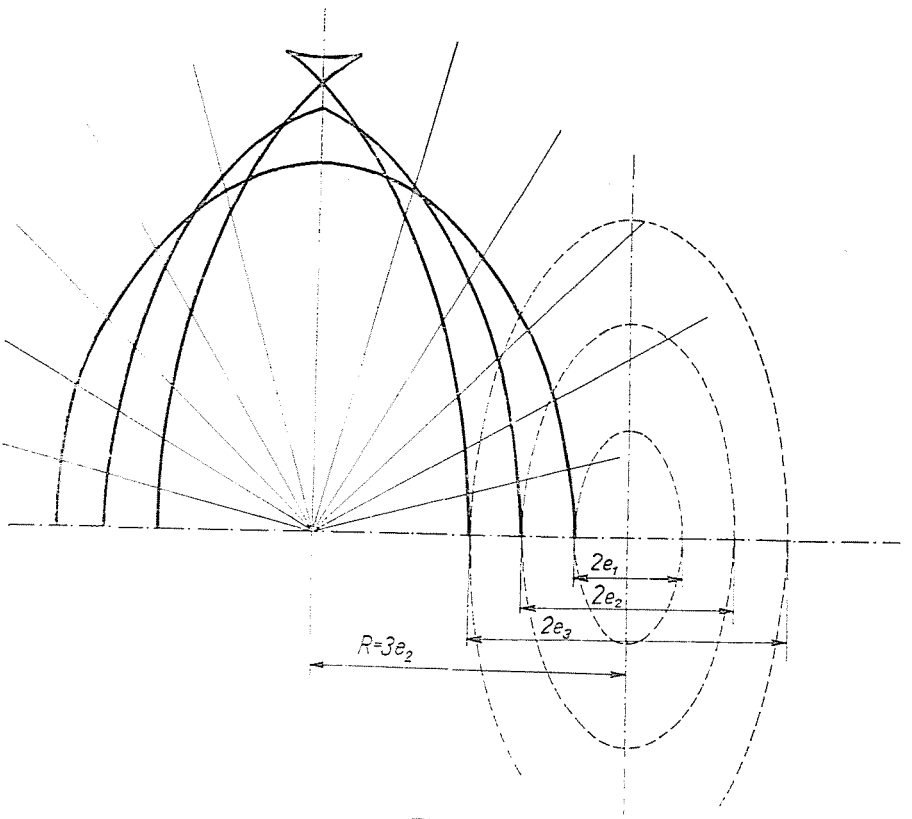

Fig. 16

The equation obtained is identical to Eq. (24) thus there are also three possibilities here :

a) when $R/e < (1 - n^2)$ [case of Eq. 19] cos $n\alpha < 1$. consequently $2n$ cusps will result for each ratio R/e. The stone has dead center positions at these spots.

b) when $R/e = (1 - n^2)$ [case of Eq. 20] cos $n\alpha = 1$, whence $n\alpha = 0^\circ + a\pi$. The curve has three cusps at the spots of maximum radii.

c) when $R/e > (1 - n^2)$ [case of Eq. 21] the curve has no cusp.

Thus computation has justified the conclusions drawn from Fig. 15.

Figures 8, 9, 10 show sets of curves. In Fig. 8 $n = 2$, here $|1 - n^2| = 3$. In Fig. 9 $n = 3$, here $|1 - n^2| = 8$. In Fig. 10 $n = 4$ and $|1 - n^2| = 15$.

In practice an answer is generally expected for the question which eccentricity should be selected for a profile of a specified mean radius R. Increasing e causes the difference between minimum and maximum radii to increase, and increasing eccentricity results in a tapering profile at any radius. Figures 16, 17 and 18 demonstrate the effect of increasing the eccentricity for the case of $R = \text{const}$.

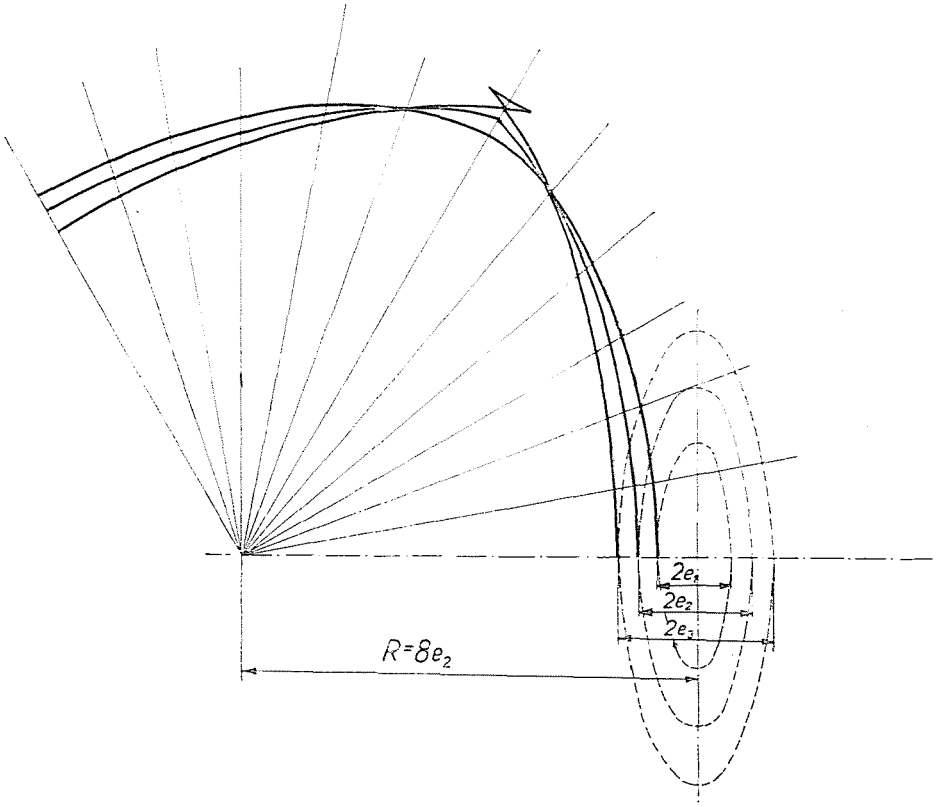

Fig. 17

The curves in each set shown in Figs. 8. 9 and 10 are equidistant, and the functions of the radii of curvature show that the centers of curvature of the extreme value spots in case of any ratio of R/e lie at the cusps of the curve. Osculatory circles to the small and the big arcs facing the former can be drawn from these cusps.

In case $n = 2$ there are two cusps only (on the major axis) from which the osculatory circle to the arc of small radius of curvature can be drawn. The centers of curvature for the extreme value spots on the minor axis of the ellipse lie at the point of intersection of this axis with the curve including the cusps (Fig. 8).

Furthermore, we have to decide the question : a polygon of how many angles should be chosen as the most suitable.

Substituting $n = 1$ in Eqs. (13) and (14) of the profile

$$x = R \cos \alpha - e$$

$$y = R \sin \alpha$$

as a result, a polygon profile of one angle is a circle with the center shifted to a distance e (eccentric). By similar substitution of $n = 2$ the result is an ellipse. A further increasing of n gives the already known polygon formation, composed of a number of n arcs.

One group of polygon profiles is characterized by constancy of dimension, *i.e.* when checking its dimension at any chosen spot the measurement result remains the same. For instance a circle has a constant dimension

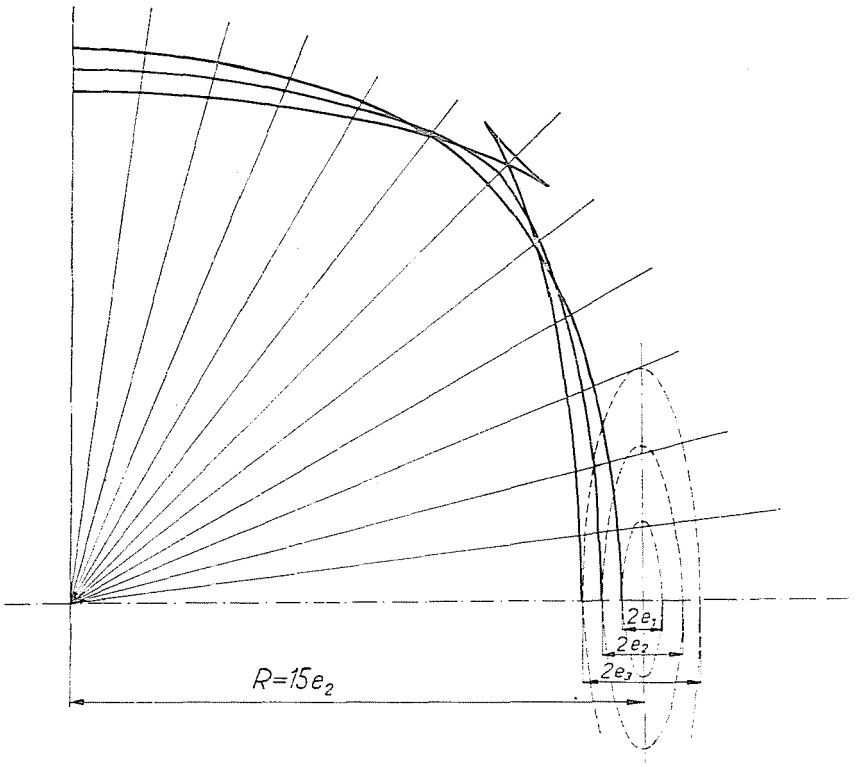

Fig. 18

whereas an ellipse has not. It is seen that this quality is not independent of the number of the polygon angles and it may be assumed that a profile is of constant dimension whenever the number of angles is an odd number.

This problem may be examined as follows :

By means of an external caliper gauge or any other device having parallel measuring surfaces, the distances between such points of the profile can be measured, the tangents of which are parallel to each other. Yet to such points belong angular displacements $n\alpha$ and $n\alpha + n\pi$, respectively.

Let n be an even number : Fig. 19 demonstrates that while the driving eccentric rotates through an angle $n\alpha$, the working point of the stone arrives at position A. The point on the workpiece which is processed at this instant by the stone can be determined by turning off the triangle OAA_1 by an angle α. The point on the profile is A', the direction of the tangent $A'A'_1$. When the angular displacement of the driving eccentric grows to $n\alpha + n\pi$, the working point on the stone again coincides with point A. Point A'' on the workpiece can be determined by turning the triangle OAA_1 through an angle

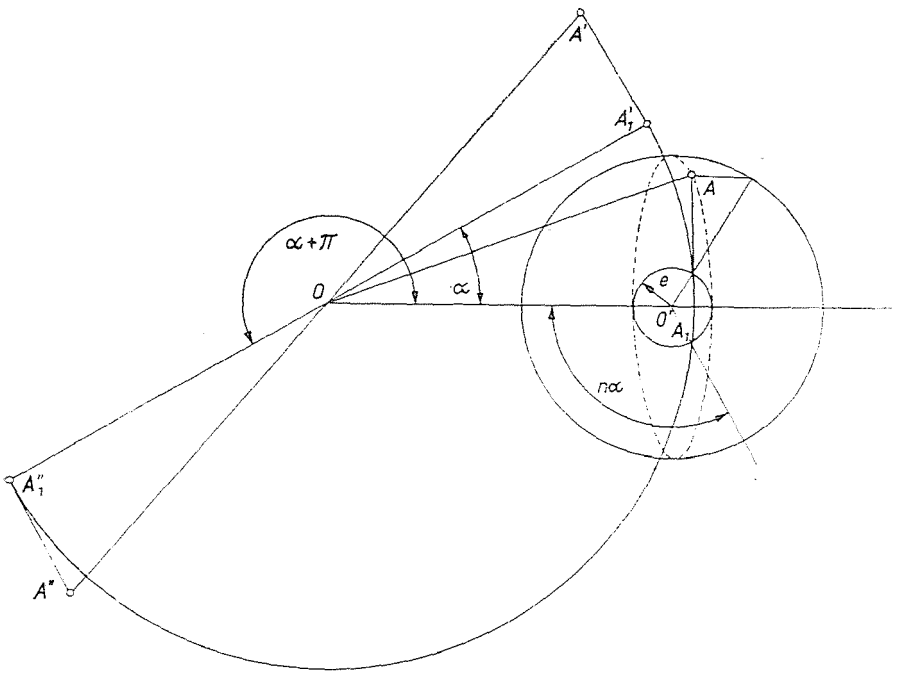

Fig. 19

$\alpha + \pi$. The tangent to point A'' directed along $A_1''A''$ is parallel to the tangent to point A'. The distance measured is $\overline{A'_1A''_1}$. The distance $\overline{OA_1'}$ can be expressed as

$$\overline{OA_1} = R + e \cos n\alpha$$

$$\overline{A_1'A_1''} = 2\overline{OA_1} = 2\,(R + e \cos n\alpha) \qquad (26)$$

It can be seen that the distance measured is a function of α, and therefore in case when n denotes an even number, the profile cannot possibly be of constant dimension.

Now let n be an odd number. By following the construction in Fig. 20, we see that at an angular displacement $n\alpha$ the working point on the disc comes to position A, and at an angular displacement $n\alpha + n\pi$ to position B. The points on the profile can be determined by turning off the triangles OAA_1 and OBB_1. The points on the profile are A' and B', the directions of the tangents t and t', the measured distance $\overline{A'B'}$.

$$\overline{A'B'} = \overline{A_1'B_1'}$$

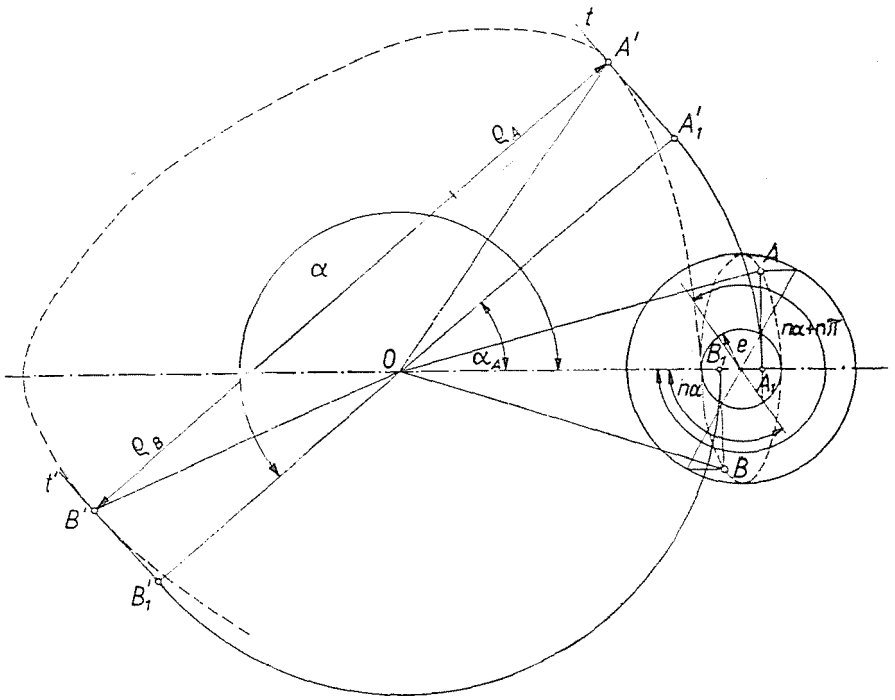

Fig. 20

and

$$\overline{A_1'B_1'} = \overline{OA_1'} + \overline{OB_1'}$$

where

$$\overline{OA_1'} = R + e \cos n\alpha$$

and

$$\overline{OB_1'} = R + e \cos (n\alpha + n\pi)$$

since

$$\cos n\alpha = -\cos (n\alpha + n\pi)$$

hence

$$\overline{OB_1'} + \overline{OA_1'} = 2R \qquad (27)$$

This order of ideas applies to any angle $n\alpha$. It follows that polygon profiles with odd numbers of angles have a constant dimension, identical with the mean diameter. Also the sum of the two radii of curvature at points A' and B' is equal to the mean diameter, since

$$\varrho_{A'} = R - e\,(1 - n^2)\cos n\alpha$$

$$\varrho_{B'} = R - e\,(1 - n^2)\cos\,(n\alpha + n\pi)$$

whence

$$\varrho_{A'} + \varrho_{B'} = 2R$$

This analysis advocates for application of polygon profiles with odd numbers of angles, because a constant dimension renders assembling and gauge testing of the pieces simple, furthermore such profiles are self-centering. Out of the polygon profiles with odd numbers of angles, the case $n = 1$ gives a profile unsuitable for connection, thus $n = 3, 5, \ldots$ etc. can be taken into consideration.

If we possess two specified profiles of identical dimensions, one with $n = 3$ and the other with $n = 5$ as number of angles, the question is, which number of angles is more serviceable in practice can readily be answered. Provided the eccentricity is the same for both cases, the minimum nominal radius where no cusp is produced will be $R = 9e$ for $n = 3$, and $R = 25e$ for $n = 5$. Thus, if the nominal diameter of the profile is $25e$ minimum radii of curvature will be

$$\text{for } n = 3 \qquad \varrho_{\min} = [25 + (1 - n^2)]\,e = 17e, \text{ and}$$

$$\text{for } n = 5 \qquad \varrho_{\min} = [25 + (1 - n^2)]\,e = e$$

i.e. other things being equal, the increase of the number of angles results n a very substantial reduction of the minimum radius of curvature.

This fact is particularly important for the processing of inner profiles. Namely, inner profiles can also be produced by broaching, yet, if an execution of high accuracy is needed, or production of a pull broach is not economic, the inner surface has to be ground (a hardened surface cannot be finished by broaching, either, but only by grinding). What was said holds true also for processing inner surfaces, yet the maximum diameter of the disc is limited :

$$d_{\max} \leq 2\,\varrho_{\min} \quad \text{(Fig 21}a\text{ and 21}b\text{)}$$

where

$$\varrho_{\min} = \left[\frac{R}{e} + (1 - n^2)\right] e$$

This condition sets an upper limit to the grinding disc diameter, whereas the lower limit results from the conditions of metal cutting.

The above considerations demonstrate that the most serviceable are polygon profiles of three sides.

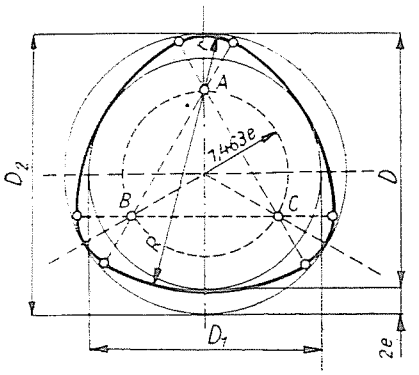

Fig. 21a

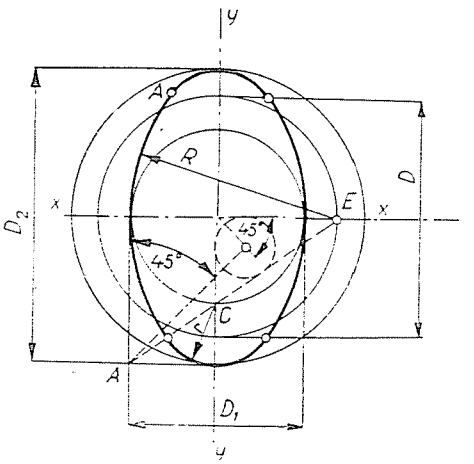

Fig. 21b

So as to render representation simpler, we have delineated the profiles as composed of arcs. The course of the construction runs as follows (Fig. 22a) : Draw a circle of a radius 7,643e. This circle intersects the radii inclined at 120° to each other. From these points, the arcs of radii r and R can be drawn. These arcs meet on the straight lines joining the points A, B and C. (An approximate construction method for elliptical profiles is shown in Fig. 22b.)

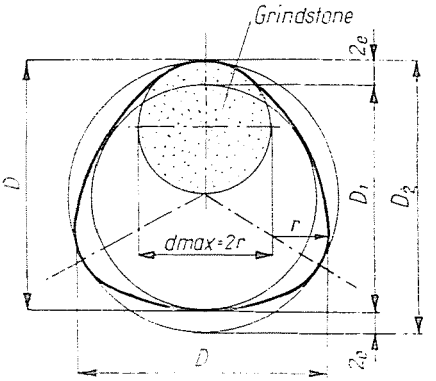

Fig. 22a

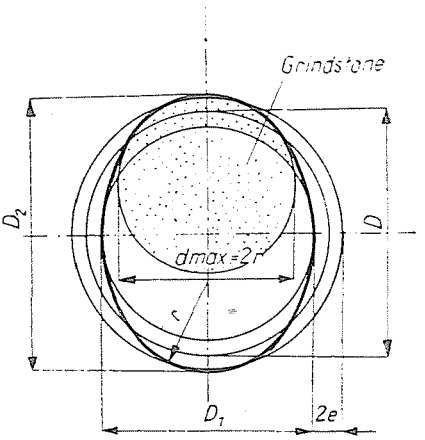

Fig. 22b

Generating polygon profiles with epicyclic gear

The same profile can also be produced by a rolling movement. It is known that when inside a stationary circle of radius R another circle, of radius $R/2$, rolls without sliding, the points on any chosen diameter of the rolling circle move on elliptical paths, with the exception of the points lying on the circumference and the centre of the small circle, the paths of which degenerate in a straight line and a circle, respectively (Fig. 23). A point at a distance a from the center of the rolling circle describes an ellipse and by variation of the parameter $\bar{a}$ the shape of the ellipse, *i.e.* the ratio of the major and minor axes can be varied.

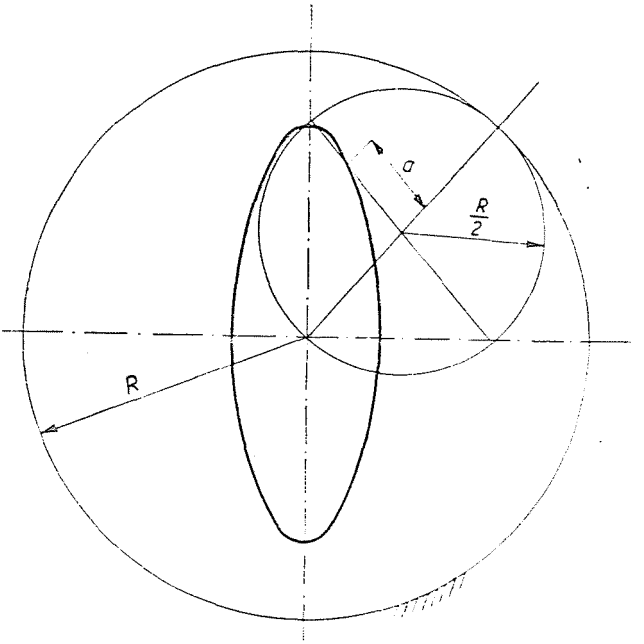

Fig. 23

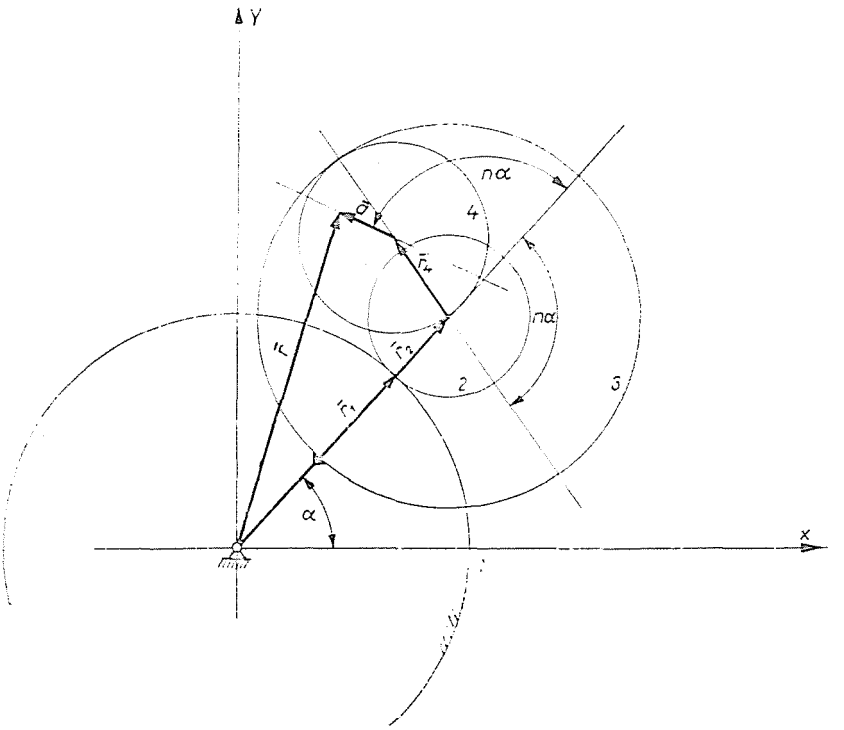

Fig. 24

The elliptical path of the stone center can also be derived from the rolling without sliding of the circle (4) inside the circle (3) (Fig. 24). $r_3 = 2\,r_4$. In case the circle of radius r_4 is not at stillstand, but rotates about a point D, then, in fact, the ellipse described by the point determined by the distance $\bar{a}$ will rotate as compared to the workpiece being at stillstand.

According to Fig. 13. we can write

$$\bar{r} = \overline{r_1 + r_2} + \bar{r}_4 + \bar{a}$$

where

$$\overline{r_1 + r_2} = (r_1 + r_2)\cos\alpha\,\bar{i} + (r_1 + r_2)\sin\alpha\,\bar{j}$$

$$\bar{r}_4 = -r_4\cos(n\alpha - \alpha)\,\bar{i} + r_4\sin(n\alpha - \alpha)\,\bar{j}$$

$$\bar{a} = a\cos(n\alpha + \alpha)\,\bar{i} + a\sin(n\alpha + \alpha)\,\bar{j}$$

substituting

$$\bar{r} = x''\,\bar{i} + y''\,\bar{j}$$

where

$$x'' = (r_1 + r_2)\cos\alpha - r_4\cos(n\alpha - \alpha) + a\cos(n\alpha + \alpha)$$

$$y'' = (r_1 + r_2)\sin\alpha + r_4\sin(n\alpha - \alpha) + a\sin(n\alpha + \alpha)$$

substituting the functions

$$\cos(n\alpha - \alpha) = \cos n\alpha\cos\alpha + \sin n\alpha\sin\alpha$$

$$\sin(n\alpha - \alpha) = \sin n\alpha\cos\alpha - \cos n\alpha\sin\alpha$$

$$\cos(n\alpha + \alpha) = \cos n\alpha\cos\alpha - \sin n\alpha\sin\alpha$$

$$\sin(n\alpha + \alpha) = \sin n\alpha\cos\alpha + \cos n\alpha\sin\alpha$$

after transposition we get

$$x'' = (r_1 + r_2)\cos\alpha - (r_4 - a)\cos n\alpha\cos\alpha - (r_4 + a)\sin n\alpha\sin\alpha \quad (28)$$

$$y'' = (r_1 + r_2)\sin\alpha - (r_4 - a)\cos n\alpha\sin\alpha + (r_4 + a)\sin n\alpha\cos\alpha \quad (29)$$

A comparison of the above equations with those of the polygon profile:

$$x = R\cos\alpha - e\cos n\alpha\cos\alpha - n\,e\sin n\alpha\sin\alpha$$

$$y = R\sin\alpha - e\cos n\alpha\sin\alpha + n\,e\sin n\alpha\cos\alpha$$

suggests the values to be selected for the radii r_1, r_2, r_3 and r_4 of the circles and for the distance a. These values are determined through the following relationships :

$$R = r_1 + r_2$$

$$e = r_4 - a$$

$$n\,e = r_4 + a$$

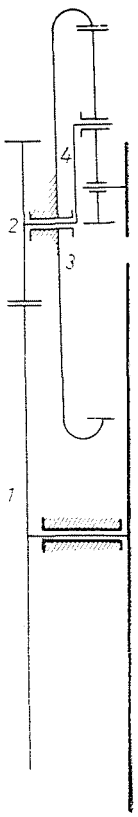

Fig. 25

moreover, $r_1 = n\ r_2$, transformation gives

$$n\,e + e = 2r_4$$

$$n\,e - e = 2a$$

From these relationships the parameters of the epicyclic gear can be determined.

The sketch of the epicyclic gear is given in Fig. 25. In case the whole system rotates with an angular velocity $-\omega_3$ the wheel (3) comes to a stillstand, the workpiece rotates about its own axis, and only the axis of the grinding stone has the swinging motion, discussed above. The shaft of the grinding disc has to be mounted in the wheel (4) in such a way that it could be shifted radially. For each number of polygon angles the distance $\bar{a}$ can be determined:

$$\begin{aligned} \text{if} \quad n &= 1, & a &= 0 \\ n &= 2, & a &= {}^1/_3\ r_4 \\ n &= 3, & a &= {}^1/_2\ r_4 \\ n &= 4, & a &= {}^3/_5\ r_4 \end{aligned}$$

Processing polygon profiles with apparatus to be mounted on grinding machine

To transform a grinding machine in hand is a rather difficult task, because the shaft of the grinding stone is mounted in bearings set in the frame. In a polygon grinding machine the shaft of the stone has a swinging motion, whereas the axis of the workpiece is at stillstand. The idea arises that the two motions could be interchanged. In order to generate the desired profile, a relative motion between workpiece and stone is needed. This can come about also when the axis of the workpiece has a swinging motion and only the stone rotates about its own axis (Fig. 26).

Notations in Fig. 26:

1. Grindstone,
2. Workpiece clamping head,
3. Swinging parts,
4. Driving eccentric,
5. Gear box of ratios 1 : 1, 1 : 2, 1 : 3, 1 : 4,
6. Synchronizer of workpiece and eccentric motions,
7. Multiplying lever for shifting axis of workpiece vertically,
8. Workpiece,
9. Slide for transmitting horizontal motion of eccentric,
10. Slide for transmitting vertical motion of eccentric.

The driving eccentric (4) has a kinematic connection with the workpiece (8) only. The slides (9) and (10) together with the lever (7) compel the workpiece to execute a motion similar to that of the grindstone in the polygon machine. The gear box (5) (which is only symbolically noted as a gear drive) causes the shaft of the workpiece to execute n swings at each revolution. Thus, all parts of the device constructed according to the above,

except the stone, can be assembled in one body, which can be fixed to the bench of the grinding machine.

The relative motions of the workpiece compelled to move with its axis swinging, and of the grindstone turning about a fixed axis result in the same polygon profile, the equation of which is already known.

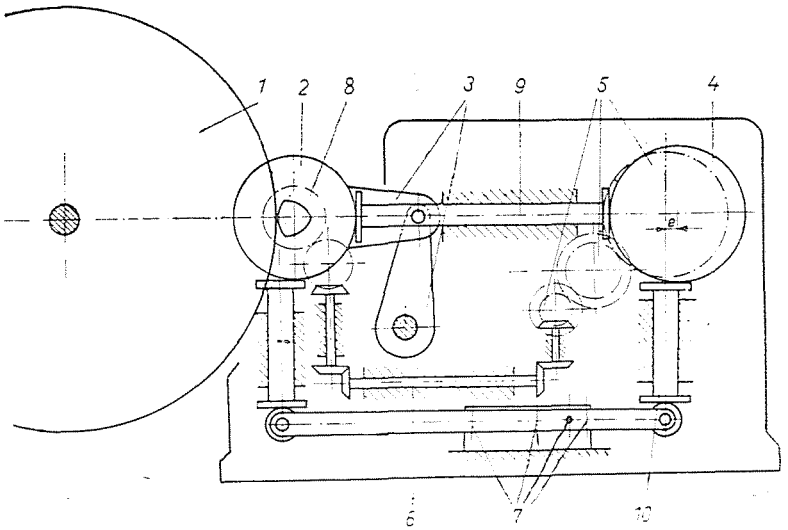

Fig. 26

Kinematic problems for generating polygon profiles have been solved in the above. It will be the task of the machine tool designer to create a proper constructional device for practiced realisations.

Summary

The above paper offers a synthetic investigation of various polygon profiles on the basis of the kinematic sketch of a polygon grinding machine, shows ways of generating polygon profiles and finally points out how such profiles can be processed by means of an equipment which can be mounted on grinding machines at disposal.

References

1. DURRENBACH, R.: Verbindungen von Welle und Nabe. Konstruktion **6**, Heft 10. 399—401 (1954).
2. Polygon Manurhin (Catalogue).

E. FILEMON, Budapest, XI., Müegyetem rakpart 3. Hungary.